Hybrid solid polymer electrolyte from diapers as separator for electrochemical double layer capacitor (EDLC)

Cite as: AIP Conference Proceedings **1972**, 020001 (2018); https://doi.org/10.1063/1.5041219

Mohd Azman Hashim, Nadhrah Md. Yatim, Nor Azura Che Mahmud, Nur Ezniera Shafieza Sazali, Ellisah Hamdan, Mohd Adib Yahya, Che Wan Zanariah Che Wan Ngah, and Syahida Suhaimi

AIP Conference Proceedings **1972**, 020001 (2018); https://doi.org/10.1063/1.5041219

Hybrid Solid Polymer Electrolyte From Diapers As Separator For Electrochemical Double Layer Capacitor (EDLC)

Mohd Azman Hashim[1,a)], Nadhrah Md. Yatim[1,b)], Nor Azura Che Mahmud[1,c)], Nur Ezniera Shafieza Sazali[1,d)], Ellisah Hamdan[1,e)], Mohd Adib Yahya[1,f)], Che Wan Zanariah Che Wan Ngah[1,g)], Syahida Suhaimi[1,h)]

[1]*Faculty of Science and Technology, Universiti Sains Islam Malaysia, Bandar Baru Nilai,*
71800 Nilai, Negeri Sembilan, Malaysia

[a)]Corresponding author: m_azman@usim.edu.my
[b)]nadhrah@usim.edu.my
[c)]nor_azuraa@yahoo.com
[d)]eznierashafieza@gmail.com
[e)]ellisahhamdan@gmail.com
[f)]mohd.adib@usim.edu.my
[g)]cw.zanariah@usim.edu.my
[h)]syahida@usim.edu.my

Abstract. EDLC was fabricated using hybrid solid polymer electrolyte from PVA-diapers and an activated carbon powder as electrode by using solution casting method. For comparison, four types of EDLC cells were constructed and tested. It was found that an EDLC with a PVA-diapers (60:40) polymer electrolyte exhibited much higher capacitance and longer cycle-life. The electrocapacitive properties of the supercapacitor (P50HD50, P60HD40, P70HD30 and P80HD20) were done using electrochemical impedance spectroscopy (EIS), cyclic voltammetry (CV), and galvanostatic charge discharge (GCD). Results from these analysis showed that P60HD40 cell had recorded excellent rate capability and highest C_{sp} value of 179 F g^{-1} (EIS), 50 F g^{-1} (CV), 328 F g^{-1} (GCD) respectively. Futher, results from ESR (GCD) analysis showed that P60HD40 composition of PVA/H_3PO_4 liquid electroyte gave a lower value of 88.05 Ω in the supercapacitor cell compared with another cells.

INTRODUCTION

The EDLC is an energy storage-based electrochemical devices which also known as supercapasitor. It offers high energy capacities, high power densities, rapid charging/discharging rates, fast energy delivery, long life cycles and environment-friendly features. EDLCs have been widely used for various applications due to the increasing demand especially for use of electric and hybrid moving vehicles [1-2]. EDLCs are generally formed by sandwiching a separator material between two electrodes where the separator act as solid electrolyte in all solid-state supercapacitors [3]. EDLCs accumulate charges by electrostatic ion adsorption to the electrode/electrolyte double-layer interfaces of high surface area conduction materials such as activated carbons equipped with a molecule-thin layer of electrolyte as the dielectric to separate charge [4-5].

Activated carbon (AC), a kind of carbonaceous material is a feasible material for the storage of energy, particularly for electrochemical purposes due to its unique surface characteristics which are greatly influencing the EDLC performance [6]. AC is chosen as electrode material in EDLC due to its large microporosity (pore size < 2 nm), high specific surface area (1000–2500 m^2 g^{-1}) and provides cost effectiveness [7]. Aqueous as well as organic electrolyte solutions are used for their assembly. Replacing liquid electrolytes by solid polymer electrolytes is especially useful due to easy handling as it enhances the safety of supercapacitors, as it can solve problems associated with electrolyte

Recent Advancement on Applied Physics, Industrial Chemistry and Chemical Technology
AIP Conf. Proc. 1972, 020001-1–020001-9; https://doi.org/10.1063/1.5041219
Published by AIP Publishing. 978-0-7354-1679-6/$30.00

leakage and corrosion [8]. A driving force in the intense investigation and development of new polymeric electrolytes is improving due to their potential applications in various electrochemical devices, energy conversion by fuel cells, electrochromic windows and analog memory devices. Much attentions are focused on investigating the polymer electrolytes by using blending of polymers, cross-linking, insertion of ceramic fillers, and plasticization method [9]. Among the various methods of producing high ionic conduction, polymer blends are the valid and feasible approach.

In the present work, a flexible hybrid solid polymer electrolyte from diapers was prepared by adding H_3PO_4 to PVA, and a solution casting method was assembled using the solid hybrid polymer from diapers as electrolyte and separator, activated carbon as electrode. Diapers is chosen due to the performances of the fabricated EDLC cells have been evaluated by using electrochemical impedance spectroscopy, cyclic voltammetry, and galvanostatic charge-discharge techniques.

METHODOLOGY

Electrolytic Materials

An aqueous polyvinyl alcohol (PVA) solution was prepared by dissoving 2 g of PVA with 50 ml distilled water in the ratio of approximately 1:10 by volume. This solution was mechanically agitated by magnetic stirrer at 60 °C for five hours to obtain a well mixed homogenous solution. H_3PO_4 was then mixed with the PVA aqueous solution in the ratio of 80:20, 70:30, 60:40 and 50:50 wt. % as shown in Table 1. After the mixture cools down to a room temperature, the resulting slurry solution of PVA/H_3PO_4 was cast over a plastic petri dish. This was performed, after a diapers (Mamy Poko Extra Dry Unicharm brand) was cut into a 6 cm × 5.5 cm (to a size that fit into the petri dish) and soaked into the segment of the solution. The period between the casting of the samples on the petri dish and its drying took about 28 days.

TABLE 1. Overall formation of the HSPE preparation.

PVA in 50 mL distilled water (g)	Quantity of H_3PO_4 (g)	Ratio of PVA to H_3PO_4	Designation
2	0.50	80:20	P80HD20
2	0.86	70:30	P70HD30
2	1.33	60:40	P60HD40
2	2.00	50:50	P50HD50

Electrode Materials

Commercial activated carbon (Carbon 50) of reasonable pore-size distribution was selected for this study. The electrodes were pressed from a combination of 70 wt % of activated carbon and 30 wt % of polyvinylidene floride (PVDF). A 20 mL of acetone was added to the mixture in order for the solution to be easily blended in the laboratory blender. The resulting mixture of electrode was then poured in aluminium foil with a measured thickness of 2.5 μm and then dried in an oven for 24 hours at 40 °C. Two electrodes of 1 cm^2 sizes with average weight was approximately 0.004 g were built in a perspex of about 5 cm × 4 cm, the cell was set up by sandwiching two electrodes with the electrolyte (2 cm × 2 cm) and assembled in an innovative tester.

The morphological structures of the hybrid solid polymer electrolyte (HSPE) were investigated using FESEM (Hitachi model SU8030). X-ray diffraction were obtained from an X-Ray diffractometer (Bruker AXS D8) employing K_α Cu radiation of 1.5406 Å and scanned over the angular range 2θ from 0^o to 80^o. Furthermore, the electrochemical performance were carried out using EIS, CV and GCD methods. The instruments used were a Solartron 1286 electrochemical interface and a Solatron 1255 HF frequency response analyzer. The symmetrical supercapacitor cells namely Cell-1: P80HD20, Cell-2: P70HD30, Cell-3: P60HD40 and Cell-4: P50HD50 were fabricated using the respective commercial activated carbon, aluminum foils as a current collector and HSPE as electrolyte.

The specific capacitance (C_{sp}) of the samples was calculated using equation (1), (2) and (3) from the EIS, CV and GCD data, respectively.

$$C_{sp} = -\frac{1}{\pi f Z'' m} \tag{1}$$

$$C_{sp} = \frac{\oint IdV}{v.m.\Delta V} \quad (2)$$

$$C_{sp} = -\frac{2I}{m}\left(\frac{\Delta t}{\Delta V}\right) \quad (3)$$

where f is the lowest frequency, Z'' is the imaginary impedance at f, I is current (A), v is scan rate (V s^{-1}), ΔV is voltage window (V), Δt is the discharge period, ΔV is the voltage difference, I is the current density and m is the average mass (g) of the electrodes.

The specific power, P and specific energy, E were calculated from the GCD data using equations (4) and (5), respectively

$$P = \frac{VI}{m} \quad (4)$$

$$E = -\frac{VIdt}{m} \quad (5)$$

where V is the voltage, I is the current, dt is the time change and m is average mass (g) of the electrodes.

RESULTS AND DISCUSSION

FESEM Images

In order to study the change in surface morphology of the HSPE due to addition of H_3PO_4 and diapers, the FESEM images of HSPE for (a) P80HD20, (b) P70HD30, (c) P60HD40 and (d) P50HD50 were recorded at low magnifications and are shown in Fig. 1. The micrograph corresponding to all samples, it is clearly that there is no any obvious particle that can be sited in the images, this is because they are all blended colorless reagents that were allowed to dry so nothing can be sited. Overall, the entangling nature of the images indicates the presence of the compositions in the diapers and the cited gross changes from one samples to another, indicates that the diapers soaked in the prepared compositions of the PVA/H_3PO_4 liquid electrolyte was not “well-soaked” with hybrid electrolyte before drying.

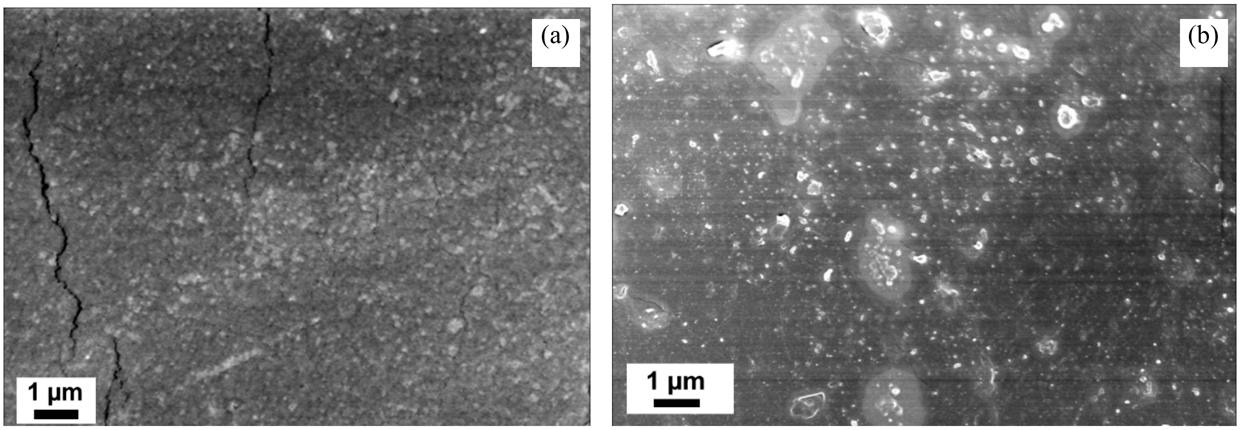

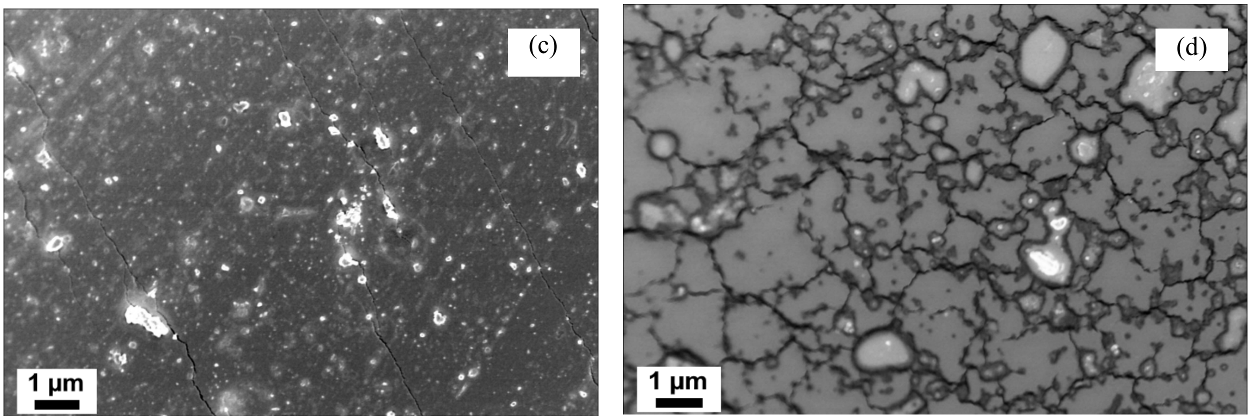

FIGURE 1. FESEM micrograph at low magnification for (a) P80HD20, (b) P70HD30, (c) P60HD40 and (d) P50HD50.

Microstructure Characterizations

Figure 2 shows the XRD spectra of the HSPE films derived from PVA/H_3PO_4. As seen in that figure, all diffraction peaks can be observed and the major diffraction peaks of the PVA/H_3PO_4 can also be clearly seen. The broad diffraction peaks that appeared at (θ =20°) is semi-crystalline peak of PVA. The addition of H_3PO_4 causes the decrease in the degree of the crystallinity and consequently the increase in the amorphicity of the material and its conductivity. While the border humps by the left shows the inclusion of the acid and that of polymer.

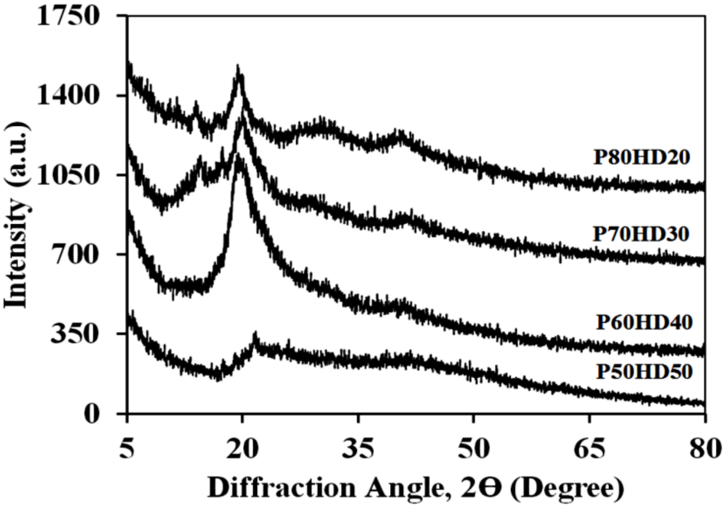

FIGURE 2. XRD spectra for all samples.

Conductivity

Conductivity measurement were carried out on the HSPE films which are also composed of all the different percentage ratio PVA-H_3PO_4 an impedance method [10]. The solid polymer films were sandwiched between a stainless steel, probe, each of surface area 2 cm^2 in radius, in a spring-loaded glass holder. The impedance measurements were carried out by using Electrical Impedance Spectroscopy (EIS) testing (Solartron 1250 electrochemical interface). The frequency range of the device was 1000 Hz - 1 MHz, and simultaneously calculating both real and imaginary impedance.

The samples exhibits Debye characteristics, and then the plots of the negative imaginary impedance versus the real impedance on the graph should be able to display a semicircle-like shape [10]. From the Eq. 6, we calculated the electrical conductivity of the samples;

$$\sigma = \frac{l}{R_b A} \tag{6}$$

where σ is the conductivity itself, l and A are the thickness and area of the samples, respectively. The thickness of the samples was measured twice at different positions of the HSPE films and average was taken using digital micrometer.

Graph of conductivity vs. percentage concentration of HSPE was plotted and shown in Fig. 3. Table 2 shows that there is a relation between the acid concentration and the polymer matrix and the conductivity is dependent on the concentration of the H_3PO_4. The thickness also give some impact on the conductivity of the samples [11].

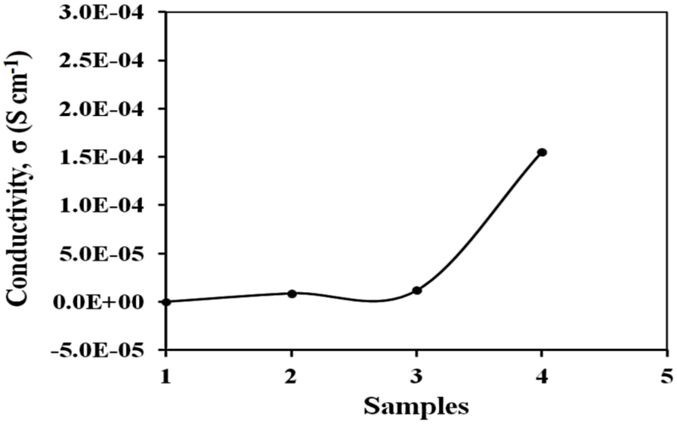

FIGURE 3. Conductivity vs HSPE samples.

TABLE 2. Parameters that determine the conductivity in HSPE.

Coding	PVA:H_3PO_4	l (cm)	Area (cm^2)	R_b (Ω)	σ (S cm^{-1})
P80HD20	80:20	0.04145	28.357	6565.5	2.23E-07
P70HD30	70:30	0.0486	28.357	192.17	8.92E-06
P60HD40	60:40	0.0349	28.357	103.45	1.19E-05
P50HD50	50:50	0.04162	28.357	9.4567	1.55E-04

Electrochemical Characterizations

Electrochemical Impedance Spectroscopy (EIS)

EIS analysis gives the fundamental understanding of the electrode/electrolyte interface behavior. The EIS data were analyzed to estimate the values of specific capacitance (C_{sp}) in different recorded frequency regions and are presented in Table 3. Figure 4 shows the typical Nyquist plots for all cells (Cell-1, Cell-2, Cell-3 and Cell-4) over a frequency range of 10^{-2} – 10^{6} Hz. The value of C_{sp} were calculated from the equation (1), the value shows that the Cell-3 have higher C_{sp} than the other cells. The decrease in C_{sp} is an indication of the existing relation between acid concentration.

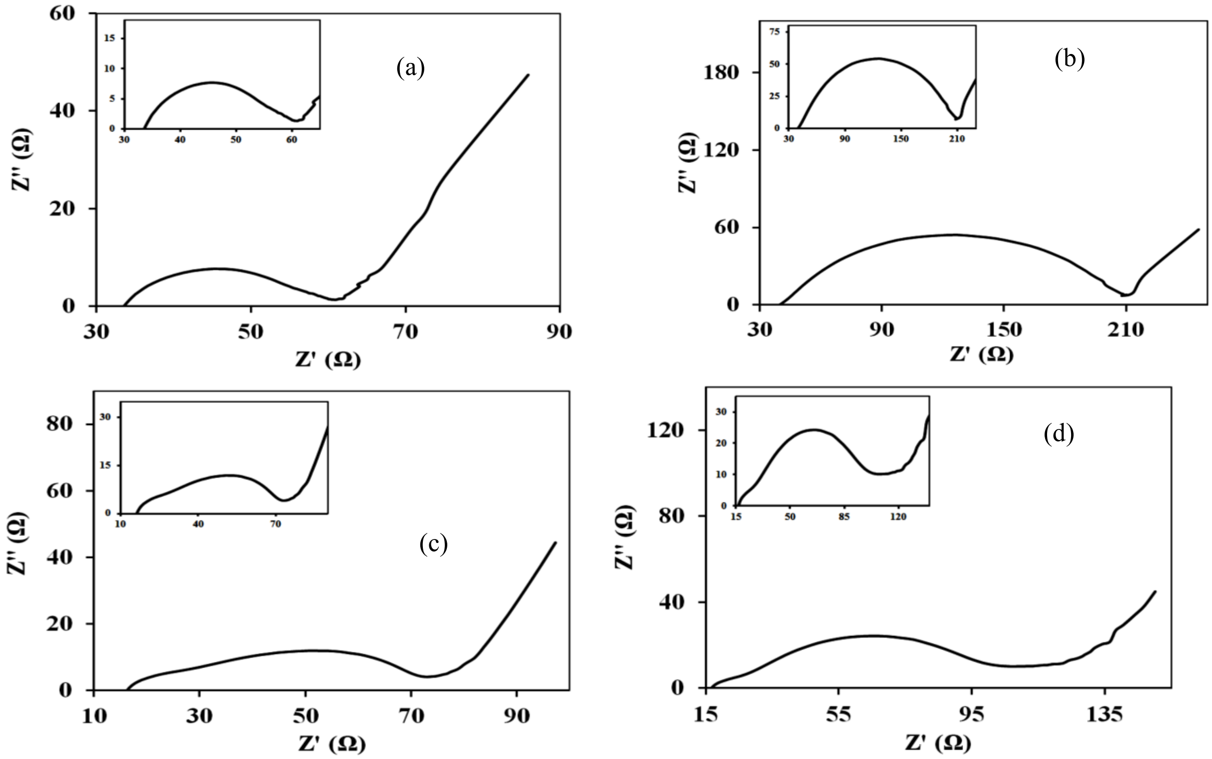

FIGURE 4. Nyquist plot for (a) Cell-1, (b) Cell-2, (c) Cell-3 and (d) Cell-4 supercapacitor cells.

Cyclic Voltammetry (CV)

Figure 5 and 6 reveals the CV of all samples at scan rates of 10, 30, 50, 70 and 100 mV s^{-1}, within a voltage window of (0.0-1.0 V) and at scan rate 50 mV s^{-1} within a voltage window of (0.0-3.0 V); respectively. It can be discerned that the resulting CV curves of the cell demonstrates a voltammogram approaching leaf-like and mirror-symmetric indicating as modest ideal supercapacitive behavior. The specific capacitance of EDLC has been enhanced drastically upon inclusion of diapers into the polymer electrolyte. The amount of mobile ions transporting absorbed within the medium could be higher with enhanced mobility which helps in improving the charge storage capacitive behavior. Higher ion concentration favors the ion migration within the hybrid polymer electrolyte and promotes the charge accumulation at the electrolyte-electrode boundary. Therefore, more free ions are drifted from an electrode to another electrode and hence absorbed onto the carbon pores forming charge accumulation at the electrode-electrolyte region. This theory explains why diapers added polymer electrolytes have higher specific capacitance. Based on the findings, inclusion of diapers is a successful way to improve the capacitive feature of EDLC.

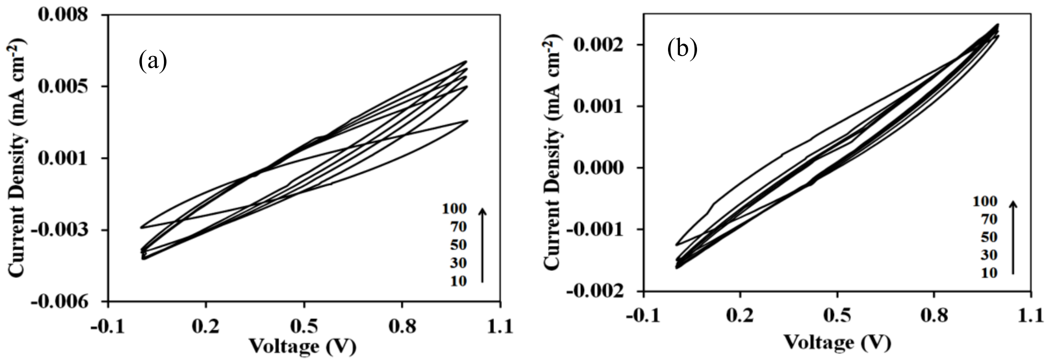

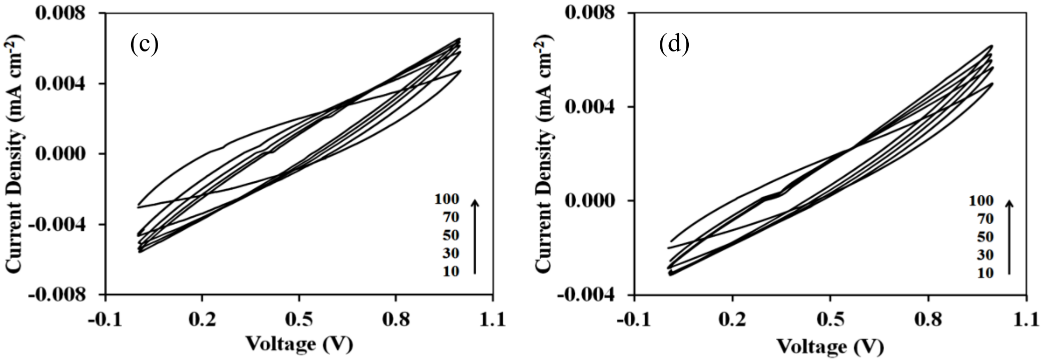

FIGURE 5. CV curves with the various scan rate for (a) Cell-1, (b) Cell-2, (c) Cell-3 and (d) Cell-4.

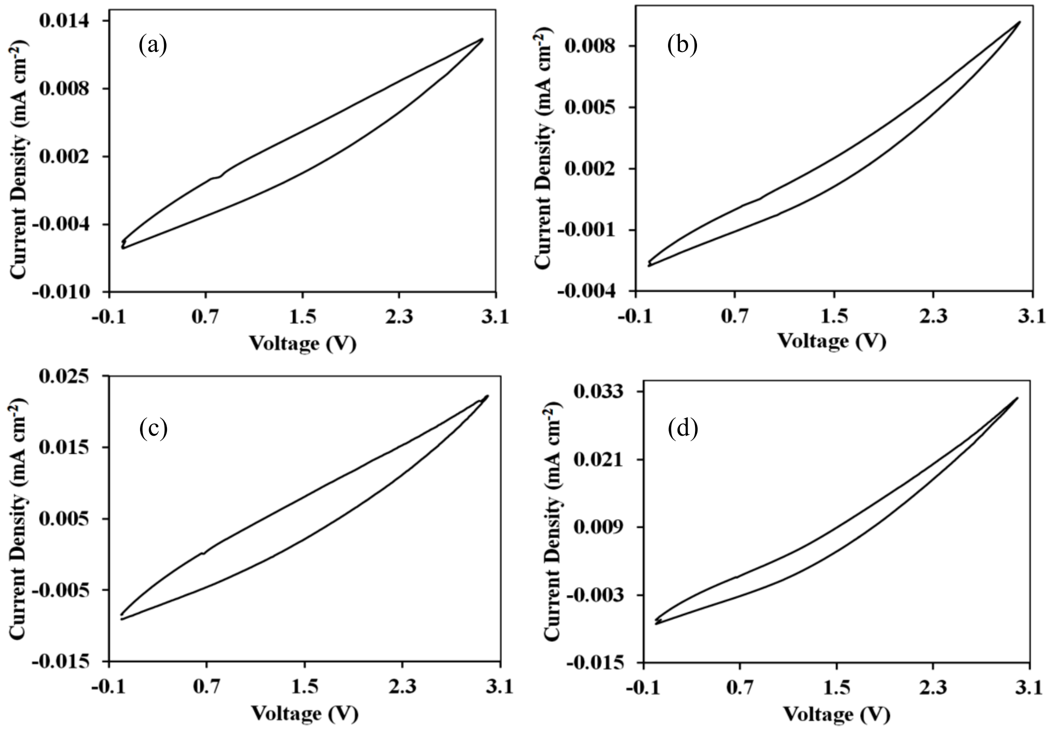

FIGURE 6. CV curves at the scan rate 50 mV s^{-1} at 3 V for (a) Cell-1, (b) Cell-2, (c) Cell-3 and (d) Cell-4.

Galvanostatic charge-discharge (GCD)

Galvanostatic charge-discharge (GCD) was used to analyze and calculate the capacitance of the EDLC samples. From the profile of the Fig. 7, the inverse V-shape of the curve with less internal resistance and voltage increment with time indicate the efficiency of the supercapacitor. The voltage–time responses behaving as a mirror-like during the charge–discharge process meant that the AC owned a good electrochemical capacitance performance [12]. The charging and discharging capacity of the supercapacitor for all cells was calculated to be 307.75, 186.30, 327.7, and 395.94 F g^{-1}; respectively.

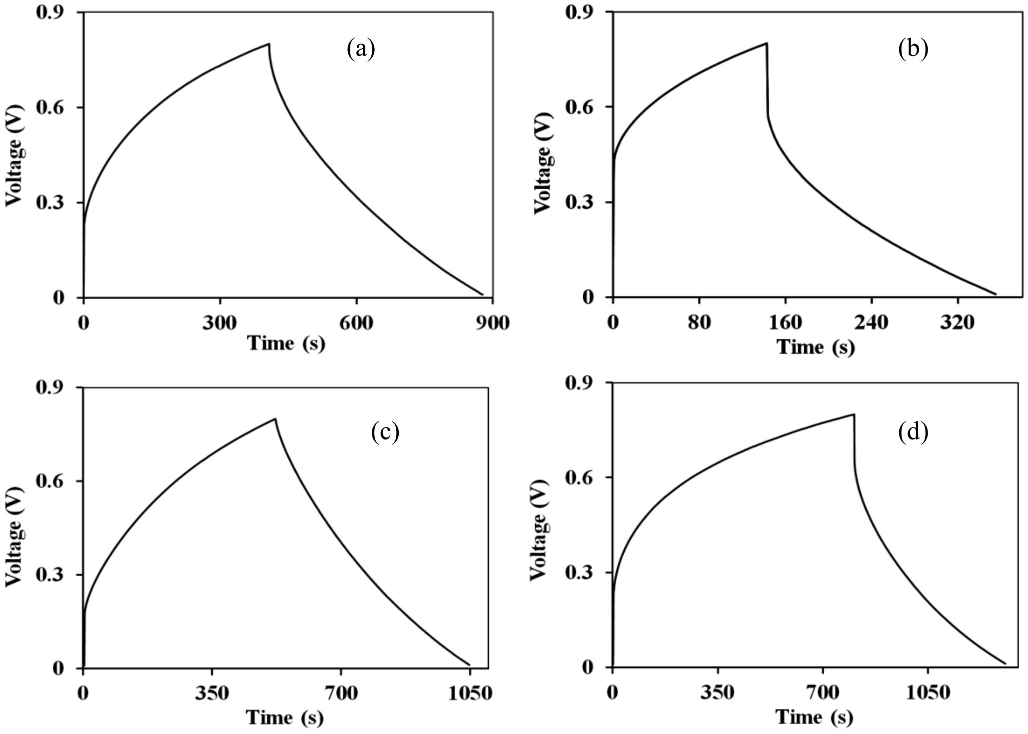

FIGURE 7. GCD curves at the current density 10 mA cm^{-2} for (a) Cell-1, (b) Cell-2, (c) Cell-3 and (d) Cell-4.

From the GCD data at 10 mA cm^{-2} at 0.8 V, the specific power, P and specific energy, E of all cells were calculated using equation (5) and (6), respectively. The results are shown as Ragone plots in Fig. 8 and are presented in Table 3.

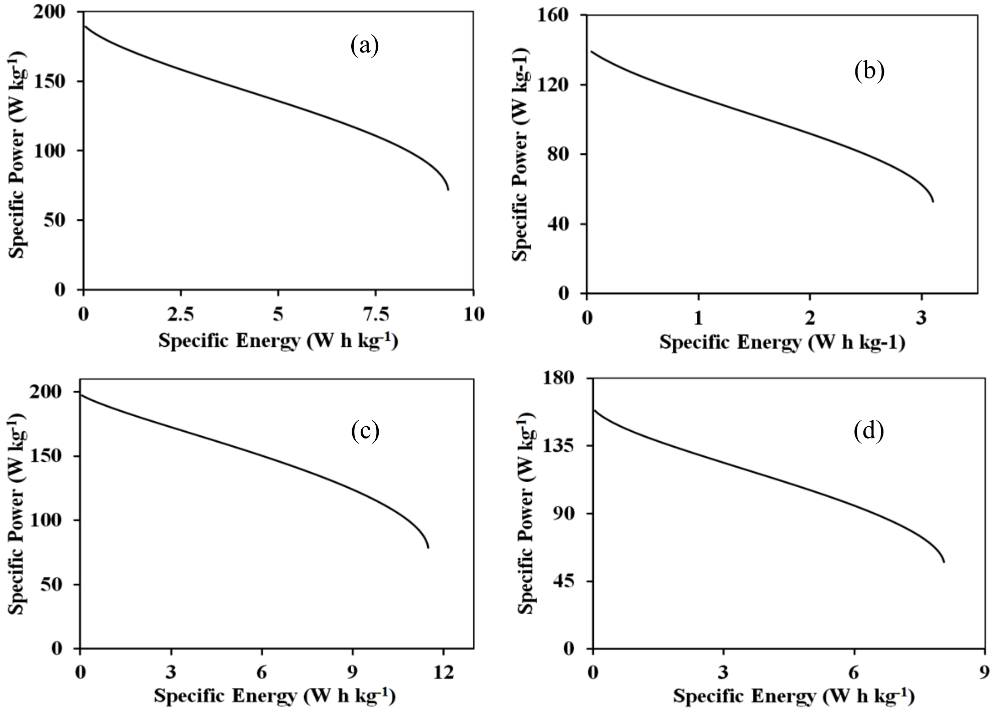

FIGURE 8. Ragone plot for (a) Cell-1, (b) Cell-2, (c) Cell-3 and (d) Cell-4.

TABLE 3. C_{sp}, E, P and ESR values for the all cells supercapacitor.

Samples	Csp (F g^{-1})			GCD		
	EIS	CV	GCD	E (W h kg^{-1})	P (W kg^{-1})	ESR (Ω)
Cell-1	167.87	27.00	327.74	9.35	189.27	84.05
Cell-2	136.15	12.96	186.47	3.10	139.10	112.51
Cell-3	179.07	49.80	335.56	11.49	197.27	2.34
Cell-4	177.10	28.53	395.39	8.07	158.43	76.76

CONCLUSION

In this work, we have explored the capacitive performance of a newly hybrid polymer electrolyte using diapers as separator for EDLC. The electrolyte was fabricated by combination of PVA/H_3PO_4 before being sandwiched with activated carbon to produce an EDLC cell. Results showed that all EDLCs exhibited good performance with high specific capacitance.

ACKNOWLEDGEMENT

The authors wish to extend their gratitude and appreciations to the management of the Pusat Pengurusan Penyedikan (PPP) USIM and Ministry of Education Malaysia (MOE) for financial support to carry out this research through Pusat Perancangan Korporat dan Pengurusan Kualiti (PPKPK) Grant Scheme (PPP/GP/PPKPK/FST/30/14815).

REFERENCES

1. W. Choi, W. Shim, D. Ryu, M. Hwang and H. Moon, Microporous Mesoporous Mater. **155**, 274–280 (2012).
2. G. Ma, J. Li, K. Sun, H. Peng, J. Mu and Z. Lei, J. Power Sources **256**, 281–287 (2014).
3. M. A. Hashim, S. R. Majid, Z. A. Ibrahim, and A. K. Arof, Ionics (Kiel).**11**, no. 5–6, 464–467 (2005).
4. D. Lee, J. Jung, M. Jung and Y. Lee, Chem. Eng. J. **263**, 62–70 (2015).
5. M. A. Yahya, C. W. Z. C. W. Ngah, M. A. Hashim, M. Ahmad, and M. A. Yarmo, Appl. Phys. Res. **7**, no. 2, 93–97 (2015).
6. M. S. Balathanigaimani, W. G. Shim, M. J. Lee, C. Kim, J. W. Lee and H. Moon, Electrochem. Commun. **10**, no. 6, 868–871 (2008).
7. C. Liew, S. Ramesh and A. K. Arof, Mater. Des. **92**, 829–835 (2016).
8. H. Yu *et al.*, Electrochim. Acta **56**, no. 20, 6881–6886 (2011).
9. S. Rajendran, M. Sivakumar and R. Subadevi, Mater. Lett. **58**, no. 5, 641–649 (2004).
10. A. S. A. Khiar and A. K. Arof, Ionics (Kiel). **16**, no. 2, 123–129 (2010).
11. M. A. Hashim and L. Sa'adu, J. Mater. Sci. Res. **3**, no. 4, 13–21 (2014).
12. Y. N. Sudhakar and M. Selvakumar, Electrochim. Acta **78**, 398–405 (2012).